Journal of the European Ceramic Society **9** (1992) 205–212

Interfacial Thermodynamics of the System Silver Chloride (Liquid)–Sapphire

U. Riedel, J. Maier

Max-Planck-Institut für Festkörperforschung, Heisenbergstr. 1, D-7000 Stuttgart 80, FRG

&

R. J. Brook*

Max-Planck-Institut für Metallforschung, Heisenbergstr. 5, D-7000 Stuttgart 80, FRG

(Received 12 July 1991; accepted 9 August 1991)

Abstract

The anisotropic wettability of liquid AgCl on selected α-Al_2O_3 surfaces ((0001), (10$\bar{1}$0), (11$\bar{2}$0)) has been determined by the sessile drop method as a function of temperature and documented by optical photography. With the contact angle obtained, the interfacial energy and interfacial entropy can be extracted and correlated with the surface crystallography of α-Al_2O_3. For the different surface planes the order of affinity is controlled—at lower temperatures—by the interaction energetics, whereas at higher temperatures the interfacial entropy becomes the controlling parameter. Cation (Ag^+) adsorption can be considered to be the driving force for the interaction process and can be correlated with the crystallography of the different planes. The experiments are completely in line with the model of 'heterogeneous doping', developed as a quantitative basis to explain conductivity effects in AgCl (solid)/Al_2O_3 composites. The wetting behavior of a glassy phase (containing Al_2O_3, SiO_2, CaO, MgO) which represents a typical composition appearing in the sintering of alumina has also been studied; the wetting is shown to be completely kinetically controlled. Nevertheless, the importance of interfacial entropy suggests a surprisingly simple explanation for the different effects of Ca^{2+} and Mg^{2+} during the sintering of alumina.

Die anisotrope Benetzbarkeit von flüssigem AgCl auf verschiedenen kristallographischen Korundflächen ((0001), (10$\bar{1}$0), (11$\bar{2}$0)) wurde mit der Methode des 'liegenden Tropfens' in Abhängigkeit von der Temperatur gemessen und photographisch dokumentiert. Mit den erhaltenen Winkeln konnte für den Kontakt AgCl (l)/Al_2O_3 die Grenzflächenenergie und -entropie abgeleitet und mit den verschiedenen kristallographischen Flächen des Korunds korreliert werden. Für die verschiedenen Oberflächen wird die Affinität—bei niedrigen Temperaturen—von der Wechselwirkungsenergie kontrolliert, während bei höheren Temperaturen die Grenzflächenentropie den bestimmenden Faktor darstellt. Als treibende Kraft des Wechselwirkungsprozesses kann die Kationenadsorption (Ag^+) angesehen werden und es läßt sich eine Korrelation mit den verschiedenen kristallographischen Ebenen ableiten. Die Experimente stehen in Einklang mit dem Modell des 'Heterogenen Dotierens', welches eine qualitative Basis für die Erklärung des Leitfähigkeitseffektes in AgCl (fest)/Al_2O_3-Mischungen darstellt. Ebenfalls untersucht wurde das Benetzungsverhalten einer Glasphase (bestehend aus Al_2O_3, SiO_2, CaO, MgO), die eine typische während des Sinterprozesses von Al_2O_3 auftretende Korngrenzenphase repräsentiert. Die Benetzung erweist sich als völlig kinetisch kontrolliert. Nichtsdestoweniger führt der allgemeine Befund der Wichtigkeit der Grenzflächenentropie bei hohen Temperaturen zu einer überraschend einfachen Interpretation des Segregationsverhaltens und der Sinteraktivität von Ca^{2+} und Mg^{2+} für die Al_2O_3-Keramikherstellung.

Le mouillage anisotrope de AgCl liquide sur des surfaces cristallographiques de α-Al_2O_3 ((0001), (10$\bar{1}$0), (11$\bar{2}$0)) a été déterminé par la méthode de 'la goutte en équilibre' en fonction de la température et documentée par photographie optique. Grâce aux

* Present address: Department of Materials, Oxford University, Parks Road, Oxford OX1 3PH.

Journal of the European Ceramic Society 0955-2219/92/$5.00

angles obtenus, l'énergie et l'entropie interfaciales ont pu être obtenues pour le contact $AgCl/Al_2O_3$ et corrélées avec les différentes surfaces cristallographiques de α-Al_2O_3. Pour les différents plans de surface l'affinité est contrôllée par les énergies d'intéraction, à de faibles températures, alors qu'à de plus hautes températures l'entropie interfaciale devient le paramètre déterminant. L'adsorption du cation (Ag^+) peut être considérée comme étant la force dominante du process d'intéraction, et peut être corrélée avec la direction cristallographique des planes. Les expérience sont en accord le modèle de 'dopage hétérogène', base quantitative pour l'explication des effets de conductivité dans les mélanges AgCl (solide)/Al_2O_3. Le comportement de mouillage d'une phase amorphe (composée de Al_2O_3, SiO_2, CaO, MgO), représentant une phase typique aux joints de grains lors du frittage de Al_2O_3, a été également étudié. Le mouillage se révèle complètement contrôlé cinétiquement. Néanmoins l'importance de l'entropie interfacial aux hautes températures conduit à une interprétation du comportement de ségrégation et de l'activité de frittage de Ca^{2+} et Mg^{2+} pour la fabrication des céramiques Al_2O_3, d'une surprenante simplicité.

1 Introduction

The interactions of the different phases in a microstructure influence many of the phenomena (for example sintering, grain growth) and properties (for example electrical and thermal conductivity) that are of most significance for fabrication and use of a material. It is therefore of great importance to understand the interfacial interactions and the factors that influence them in order to be able to control materials processing and performance. Two prominent examples which both involve alumina are considered in this paper.[1,2]

The first example is represented by the system alumina–silver chloride. By studying ionic conductivity effects in solid two-phase systems the significance of the boundary for an ionic conductor (e.g. Ag halides)[2] in terms of the interaction with a neighboring phase (such as Al_2O_3) could be clearly demonstrated.

Adding alumina to solid silver chloride results in an accumulation of the silver cations at nucleophilic oxide surface groups (Fig. 1) according to the equation

$$—OH + Ag_{Ag} \rightleftharpoons —OHAg^{\cdot} + V'_{Ag} \qquad (1)$$

where OH is taken as an example of an adsorbing

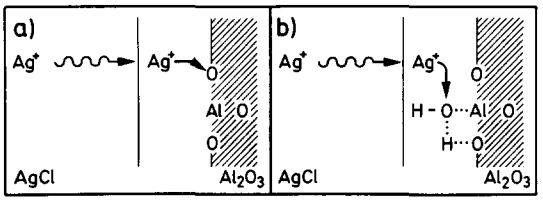

Fig. 1. Adsorption of the Ag^+ on Al_2O_3. (a) Dry; (b) hydrated, emphasizing the influence of OH groups or water.

center.[3] The increase in the mobile silver vacancy concentration in the boundary regions turns out to be the reason for the conductivity enhancement. The interaction process is analogous to the well known phenomenon of proton adsorption in aqueous solutions. Moreover, the order of efficiency ($(Al_2O_3) > (SiO_2)$) corresponds to the ranking of pH of zero charge and thus to surface acidity/basicity (γ-Al_2O_3, 9; α-Al_2O_3, 7; SiO_2, 3).[4,5] Preliminary studies show that the wetting behavior of liquid AgCl on different substrates is representative of the conductivity enhancement in the corresponding solid-state system. AgCl(l) readily penetrates a pellet of polycrystalline γ-Al_2O_3, whereas a polycrystalline aerosil (SiO_2) pellet is poorly wetted.[6] An intermediate case is α-Al_2O_3, where clearly measurable contact angles can be found.

In the present work wetting angles are determined as a function of temperature for different surface orientations to assess how well the silver adsorption can be explained by interfacial thermodynamics.

The second example relates to another scientifically and technologically important problem, namely the sintering of alumina. It is well known that, unlike CaO, MgO acts as an effective sintering aid in the alumina system.[7] This difference is attributed to the fact that MgO segregates isotropically, hence causing regular grain development,[8–10] whereas CaO is found to segregate preferentially to the prism planes[11] of α-Al_2O_3, thus leading to irregular grain growth.[12] For this reason typical (MgO-containing) grain boundary glass phases have been synthesized and studied in terms of their wetting behavior on α-Al_2O_3 surfaces.

2 Experimental

2.1 Materials

As substrates three different sapphire planes were used, namely the basal plane (0001) and the prism planes ($10\bar{1}0$) and ($11\bar{2}0$). The single crystals with the defined surfaces were either bought (prism plane: Union Carbide, Tarytown, USA) or prepared by cutting as-grown single crystals (Akzo, Ibbenbüren, FRG). During the cutting procedure correct surface

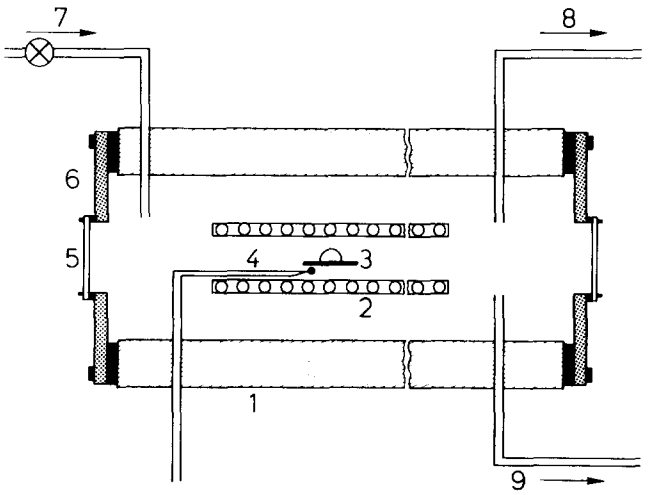

Fig. 2. The sessile drop equipment. 1, Tube furnace; 2, α-Al_2O_3 tube with Mo winding; 3, sample; 4, thermocouple (Pt/Pt, Rh); 5, quartz window; 6, closure; 7, argon inlet; 8, argon outlet; 9, vacuum pump.

orientation was ensured by the Laue technique. The crystals were polished using diamond suspensions (first 8–10 μm, then 4–8 μm). Fine polishing was performed with Syton W30 (125 nm, 30% Na_2O, pH = 10·2). Prior to the wetting experiment, the surface was treated with acetone and then with hot pure ethanol ($T = 167$°C).[13] OH groups were removed by a vacuum (0·1 Pa) anneal at 970 K for 6 h.

The Mg- and Ca-contents of the crystals were studied by atomic emission spectroscopy (ICP) and found to be below the detection limit (Mg^{2+}, $\leq 10^{-4}$ wt%; Ca^{2+}, $1{\cdot}3 \times 10^{-3}$ wt%). AgCl powder was purchased (Ventron, Karlsruhe, FRG) in the purest grade (99·999%). The glassy phases were prepared from ultrapure powders (Ventron) of α-Al_2O_3, SiO_2, $CaCO_3$ and MgO according to standard oxide mixing and melting procedures (mortar material, agate; melting crucible material, Pt). The compositions (as found by ICP) are given in Table 1.

2.2 Measurement

The wetting experiments were based on the sessile drop technique and were performed in a tube furnace, as illustrated in Fig. 2, either in air or under very reducing conditions (Mo-furnace filled with Ar after evacuation; temperature range, room temperature up to 970 K). The wetting behavior was observed by optical photography. $CaCl_2$ was used as water-getter to avoid contamination, and excess AgCl powder was present to provide a better definition of the thermodynamic state.

Illumination was avoided because of the light sensitivity of AgCl and a red security light was used where necessary. After the experiment some samples were cut and examined for possible incorporation of Ag^+ in the substrate by EDX.

Table 1. Composition of the glass phases used in the wetting studies

Sample number	*Weight percentage of*			
	Al_2O_3	SiO_2	CaO	MgO
1	36·4	32·2	27·1	0·3
2	31·6	45·4	25·3	
3	35·9	40·6	25·7	
4	35·8	35·8	27·7	00·7
5	34·5	39·5	27·1	04·1

3 Results

The photographs used in the measurements refer in all cases to the heating condition, where a stationary drop form is rapidly and reproducibly established. The contact angle, θ, remains constant for at least 10 h. The photographs have been taken after waiting periods of typically 1 min. Figure 3 shows typical photographs for sessile drops of AgCl in dry air on the $(10\bar{1}0)$ prism plane of water-free alumina. Below 725 K silver chloride is solid. At the melting point the expected drop form is observed with an angle of 65°, which decreases to a value of 35° with increasing temperature. The other planes behave qualitatively in a similar manner; the quantitative values of the angles, however, are distinctly different. In the case of alumina surfaces which have been saturated with adsorbed water the liquid AgCl spreads over the entire crystal, independent of the crystallographic plane. The results for α-Al_2O_3 do not significantly change when the contact behavior is investigated in vacuum, indicating the minor influence of the component chemical potentials. Figure 4 summarizes the results in a $\cos\theta \cdot \gamma_{AgCl}$ versus temperature plot. The angle has been measured directly from the photographs during the heating process; the values for γ_{AgCl} are taken from the literature[14,15] and are given by

$$\gamma_{AgCl} \equiv \gamma_{AgCl/g} \simeq \gamma_{AgCl/air} \simeq (208{\cdot}08 - 0{\cdot}048\,68\,T/\mathrm{K}) \times 10^{-3}\,\mathrm{Jm}^{-2}$$

It is recognized that at lower temperatures the wetting is improved in the order $(11\bar{2}0) < (10\bar{1}0) < (0001)$, whereas in the higher temperature range above 760 K the order is reversed. These results are stationary and reproducible from experiment to experiment where the heating mode is used and are independent of the initial powder morphology. In the cooling mode the wetting angle can retain a frozen-in value at least on the time scale of hours to a few days.

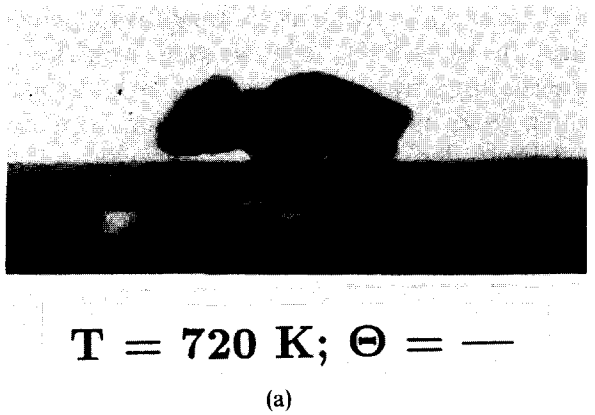

(a)

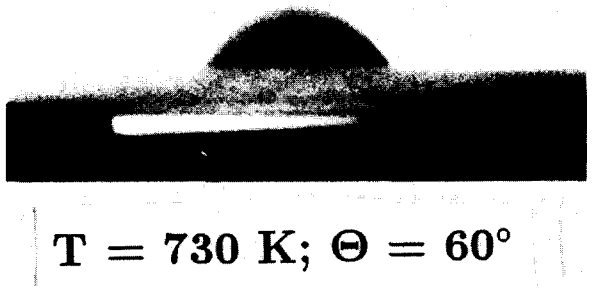

(b)

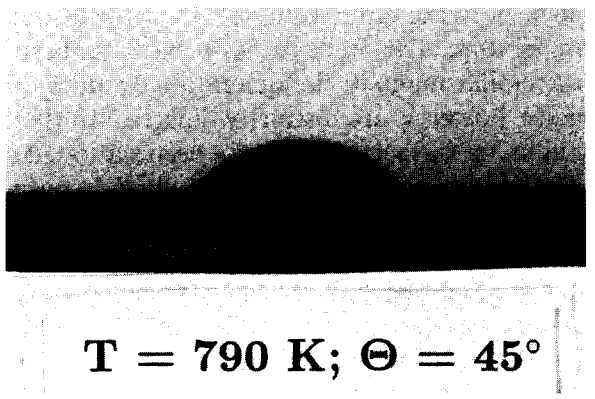

(c)

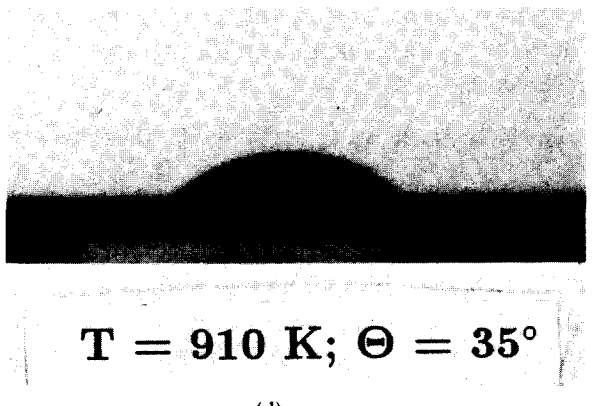

(d)

Fig. 3. Photographs of typical sessile drops of AgCl (liquid) on α-Al_2O_3 ($10\bar{1}0$) substrates at different temperatures in dry air. (a) $T = 720$ K; (b) $T = 730$ K, $\theta = 60°$; (c) $T = 790$ K, $\theta = 45°$; (d) $T = 910$ K, $\theta = 35°$.

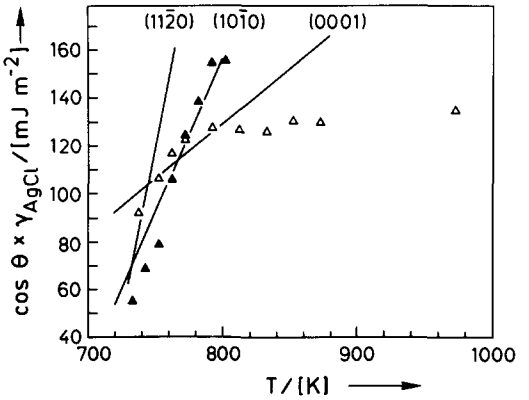

Fig. 4. Values of $\cos\theta \cdot \gamma_{AgCl/air}$ as a function of temperature. The symbols refer to the ($10\bar{1}0$) data set; filled triangles represent data under argon and open triangles data under air. (Detailed experimental data for the two other planes are in Fig. 7(a).)

The observed wetting angles for the glassy phases (containing Al_2O_3, SiO_2, CaO, MgO) are, in contrast to the AgCl case, completely kinetically controlled. Their temperature behavior is determined by the initial powder morphology rather than by the substrate under consideration, as shown in Fig. 5. A possible thermodynamic response at very high temperatures (≥ 1650 K) where the glassy drop suddenly becomes flat cannot be evaluated since $\theta \simeq 0°$. It is worth mentioning that this effect is correlated with phase changes: initially (~ 1330 K) the material is homogeneous, during heating anorthite ($CaAl_2Si_2O_8$) and gehlenite ($Ca_2Al_2SiO_7$) are precipitated (< 1650 K), and are then redissolved at still higher temperatures (e.g. 1770 K). The latter behavior is possibly responsible for the improved fluidity. No dependence of any of these features on the CaO/MgO ratio could be detected.

4 Discussion

4.1 $AgCl/Al_2O_3$

The origin of the kinetic hysteresis during cooling has not been clarified. Similar effects are known in the literature and different explanations have been given.[16] Even though the assumption of thermal equilibrium for the heating mode can be questioned by the response, a tentative thermostatic evaluation is made for those values in view of the reproducible and rapid changes in θ. In an equilibrium situation for the contact of two phases i and j the surface tension $\gamma_{i/j}$ is related to the specific free excess enthalpy $g^{ex}_{i/j}$ via

$$\gamma_{i/j} = g^{ex}_{i/j} - \sum_k \Gamma_k \mu_k \qquad (2)$$

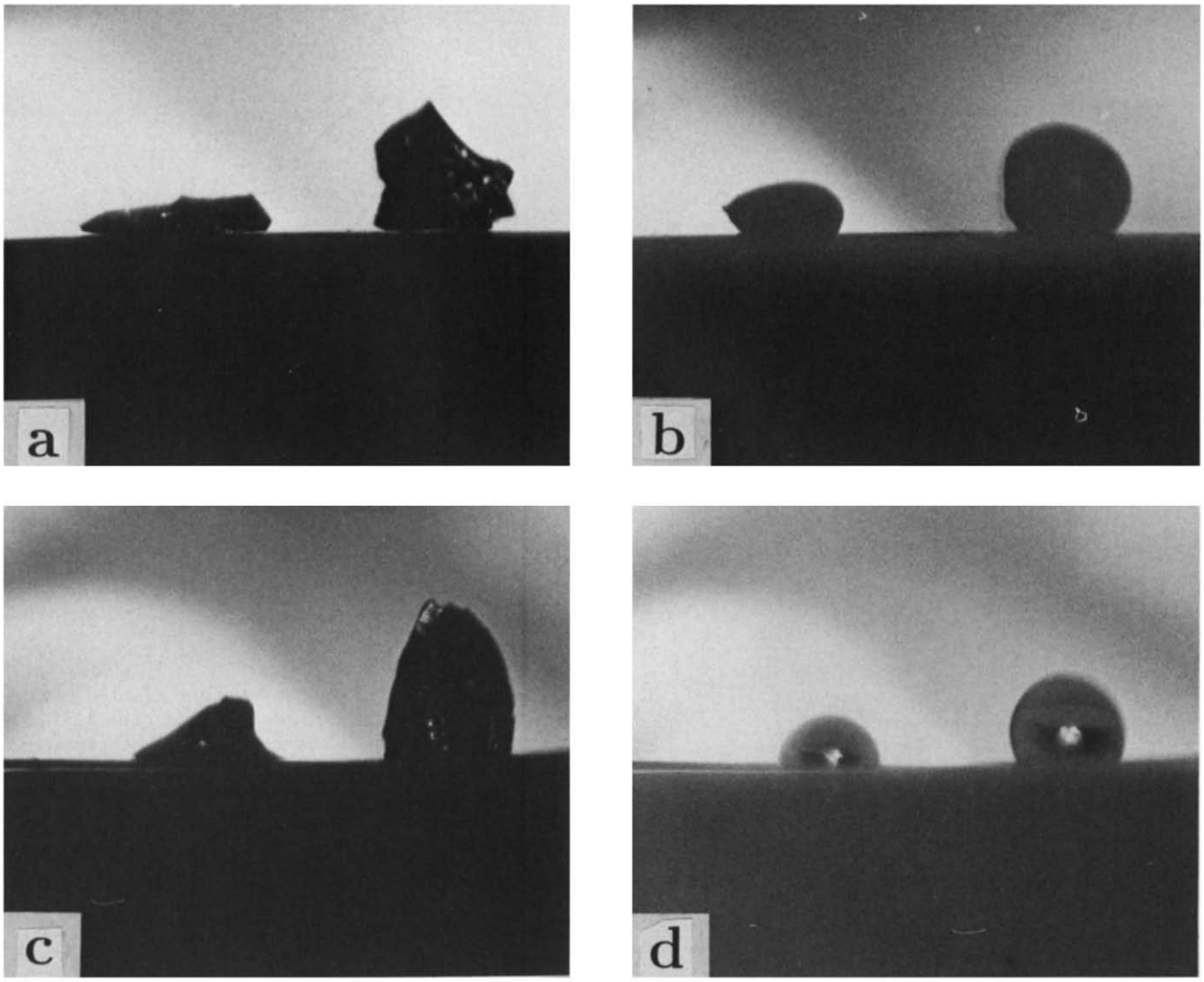

Fig. 5. The wetting behavior of the glassy phase strongly depends on the initial morphology. (a) $T \simeq 1330$ K, glassy phase with different powder morphologies on α-Al_2O_3 (0001); (b) $T = 1340$ K, the glassy phase has softened on the α-Al_2O_3 substrate, the form being roughly independent of the substrate material; (c) $T \simeq 1330$ K, glassy phase on Pt as substrate; (d) $T = 1340$ K, glassy phase on Pt as substrate.

where Γ_k and μ_k are the excess concentration and the chemical potential of k, respectively. Since the excess values refer to the complete boundary, the Γ_k values are zero in spite of possible space charge effects (Γ_k describes adsorption at the expense of the bulk concentration). As a consequence $\gamma_{i/j}$ is correlated with the (excess specific) interfacial energy $u^{ex}_{i/j}$ and the (excess specific) interfacial entropy $s^{ex}_{i/j}$ according to

$$\gamma_{i/j} = u^{ex}_{i/j} - s^{ex}_{i/j} T \tag{3}$$

Since differences between the values of the total system and the values of the idealized bulk system are involved in the analysis, the interfacial energy and the interfacial entropy can be taken as approximately independent of temperature.

Table 2. Values of $u^{ex}_{Al_2O_3(hkil)/g}$ according to the theoretical work of Tasker[17]

$u^{ex}_{Al_2O_3(0001)/g} = 2{\cdot}97\ J\ m^{-2}$	$u^{ex}_{Al_2O_3(10\bar{1}0)/g} = 2{\cdot}89\ J\ m^{-2}$
$u^{ex}_{Al_2O_3(10\bar{2}0)/g} = 2{\cdot}65\ J\ m^{-2}$	

In the sessile drop situation the surface equilibrium is described by Young's equation (l, liquid; s, solid; v, vapor):

$$\gamma_{l/s(hkil)} = \gamma_{s(hkil)/v} - \gamma_{l/v} \cos\theta \tag{4}$$

The intercepts and slopes of the plots of Fig. 4 give $u^{ex}_{Al_2O_3(hkil)/g} - u^{ex}_{Al_2O_3(hkil)/AgCl}$ and $s^{ex}_{Al_2O_3(hkil)/g} - s^{ex}_{Al_2O_3(hkil)/AgCl}$, respectively. Neglecting any influence of the gas phase, the values of $u^{ex}_{Al_2O_3(hkil)/g}$ can be taken from the theoretical work of Tasker[17] (see Table 2).

For the entropy a mean value is assessed for all planes from a γ-measurement of polycrystalline α-Al_2O_3 at 2120 K.[18] Following Tasker[17] and taking the mean u-value as $2{\cdot}6\ J\ m^{-2}$ (corresponding to the

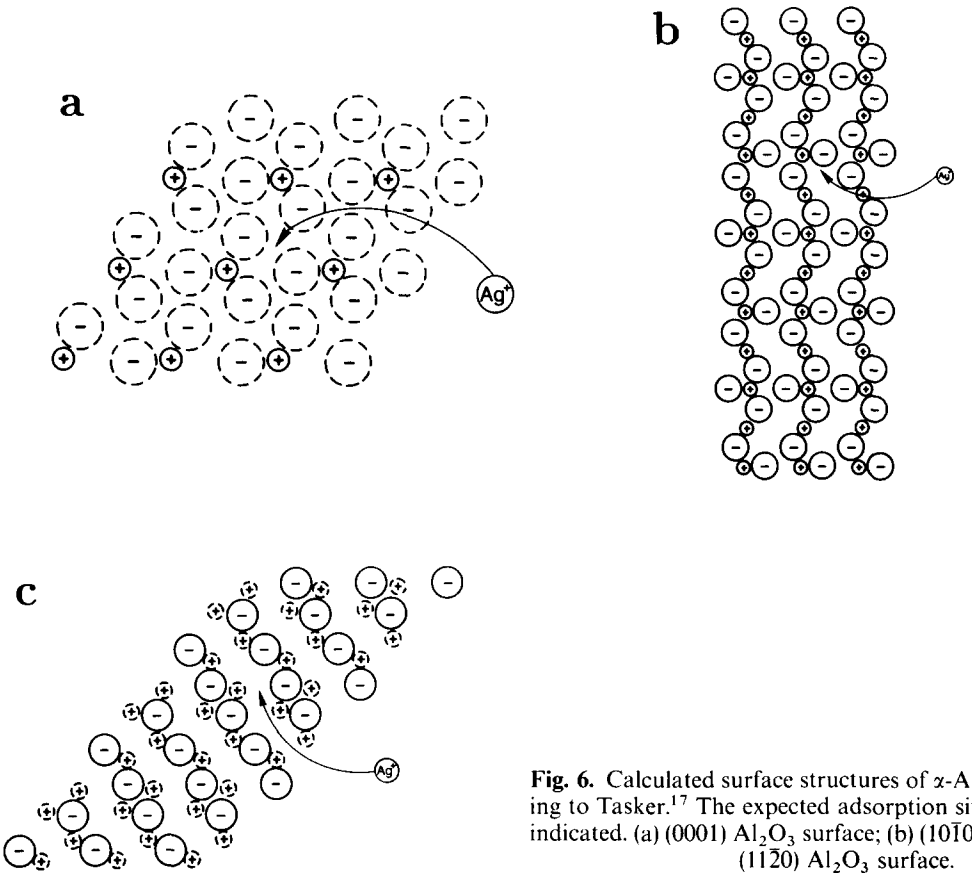

Fig. 6. Calculated surface structures of α-Al_2O_3 (0001) according to Tasker.[17] The expected adsorption site of an Ag^+ ion is indicated. (a) (0001) Al_2O_3 surface; (b) (10$\bar{1}$0) Al_2O_3 surface; (c) (11$\bar{2}$0) Al_2O_3 surface.

energetically most favored plane), a mean entropy value of $8 \times 10^{-4}\,J\,m^{-2}\,K^{-1}$ is derived. It can be shown that the error involved in the choice of the u-value as well as in the neglect of the anisotropy does not seriously affect the result of the analysis. The variations from plane to plane in the absolute values of $\gamma_{Al_2O_3(hkil)/g}$ are small (compared to the differences in $\gamma_{l/s}$).

Figure 4 shows that for $T < 760\,K$ the wetting is improved in the order (11$\bar{2}$0) < (10$\bar{1}$0) < (0001) as suggested by previous experiments,[6] whereas at higher temperatures the order is reversed. It is worth mentioning that the $\gamma_{l/v}\cos\theta$ function does not simply reflect the change of the free wetting energy as suggested by a naive consideration in terms of Dupré's specific work of adhesion. This is shown in the Appendix. Initially the curves in Fig. 4 are roughly linear, as postulated by eqns (3) and (4). At higher temperatures the $\cos\theta \cdot \gamma_{AgCl/v}$ function becomes very flat in all examples. Evaluating the linear branch as described previously, the interaction enthalpies and entropies given in Table 3 are derived.

The change in the interaction energy from plane to plane now correlates with the Ag^+ adsorption model. The lowest u-value is found for the basal plane, where extended negatively charged clusters exist according to the modeling (see Fig. 6) and favor cation adsorption. This is in striking contrast to the planes (10$\bar{1}$0) and (11$\bar{2}$0). The differences between the energy values of these two planes may be understood from similar considerations as shown in Fig. 6. The consequences for the free interaction energy are illustrated in Fig. 7, where $\gamma_{Al_2O_3(hkil)/AgCl(l)}$ is calculated for the whole T-range and extrapolated on the basis of the 740–780 K data to low temperatures. As the $\gamma_{AgCl/v} \cdot \cos\theta$ functions change in order at higher temperature, so does the (virtual) γ_{ls} in Fig. 4 ($T >$ 725°C). This reflects the influence of the interaction

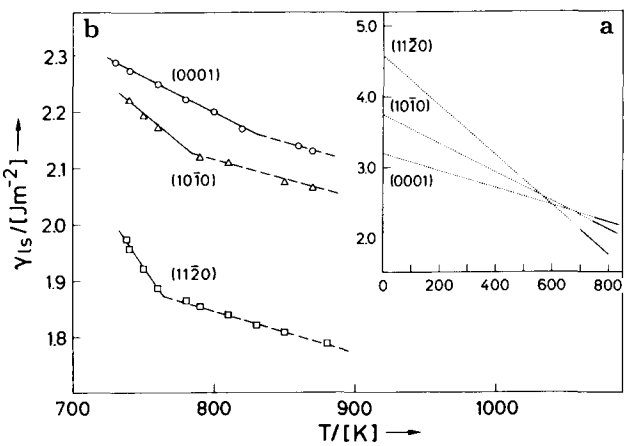

Fig. 7. The surface tension $\gamma_{s/l}$ for the different α-Al_2O_3 planes as a function of temperature. (a) The high-temperature data; (b) the extrapolation to low temperatures to indicate the influence of the energy.

Table 3. Calculated enthalpy and entropy values

(*hkil*)	u^s_{is} ($J m^{-2}$)	s^s_{is} ($10^{-4} J m^{-2} K^{-1}$)
(0001)	$3{\cdot}21 \pm 0{\cdot}5$	13 ± 2
$(10\bar{1}0)$	$3{\cdot}75 \pm 0{\cdot}6$	21 ± 3
$(11\bar{2}0)$	$4{\cdot}58 \pm 0{\cdot}7$	35 ± 5

entropy, which is often neglected in such considerations. The reverse order of the entropy contribution to γ (see Table 3) can be understood from the density of the surface structure. Whereas in the (0001) plane an adsorbed cation is expected to have few degrees of freedom, the $(11\bar{2}0)$ plane, for example, allows more pronounced configurational and vibrational contributions. The dashed lines in Fig. 7 represent the values derived from the high-temperature branch in the $\gamma_{l/v} \cdot \cos\theta$ plots. Since reconstruction of the surface in this temperature range is not expected and since the vapor pressure of AgCl is also rather low, the shift in slope may be due to saturation effects.

In agreement with the conductivity measurements, where surface groups such as OH^- or physisorbed water turn out to be effective centers, water on the alumina crystals immediately leads to complete wetting by AgCl(l). An explanation of the anisotropy of the dehydrated surfaces also in terms of different densities of residual OH groups, however, is improbable in view of the fact that the results are essentially the same for the two techniques applied (dry air, argon after evacuation).

As noted earlier, the non-equilibrium nature of the contact angles between the glassy grain boundary phases and the sapphire surfaces cannot at these temperatures be used to extract direct information either on the segregation behavior of CaO or MgO or on their sintering effects. Fortunately the results of the AgCl experiments can be used to throw some light on this problem.

As shown, the interaction entropy is expected to play an essential role at higher temperature, especially at the very high sintering temperatures necessary for Al_2O_3. Since the entropy of interaction should sensitively depend on the ion radius (see preceding arguments), the behavior of Ag^+ ($r_{Ag^+} \simeq r_{Ca^{2+}} \simeq 1{\cdot}1$ Å) may serve as a guide. Strikingly, the segregation behavior of Ca^{2+} described in literature, namely (prism plane) > (basal plane), coincides with the wetting behavior of Ag^+ at higher temperatures. In the same context, the finding that Mg^{2+} does not show preferential segregation and, even more, that small Mg^{2+} admixtures destroy the segregation anisotropy can be explained by noting that the radius of Mg^{2+} ($r_{Mg^{2+}} = 0{\cdot}8$ Å) is distinctly lower than that of Ca^{2+} (or Ag^+) and its adsorption is less influenced by the availability of preformed adsorption centers. Moreover, it is more likely that small cations such as Mg^{2+}, Ni^{2+}, Zn^{2+}, etc., may easily enter at least the first atomic layers (in all orientations) to form spinel-like surface structures (tetrahedral arrangements), resulting in the observed loss of segregation preference.

5 Conclusion

With the sessile drop method the contact angle between liquid AgCl and solid α-Al_2O_3 crystals has been measured in the temperature range between 725 and 970 K for different crystal orientations ((0001), $(10\bar{1}0)$ and $(11\bar{2}0)$). Using Young's equation, the values of the surface tension γ_{AgCl/Al_2O_3}, the interfacial energy $u_{i/j}$ and the interfacial entropy $s_{i/j}$ can be evaluated for the different planes.

It is shown that the interfacial energy controls the order of wettability ((0001) > $(10\bar{1}0)$ > $(11\bar{2}0)$) at lower temperatures, whereas the interfacial entropy is responsible for a change in behavior at higher temperatures. Consideration of the structural surface models suggests that the graduation of the values can be interpreted by Ag^+ adsorption. The results in the lower temperature range support the model of 'heterogeneous doping' for conductivity effects in ionic conductor/insulator composites.

A possible explanation for the segregation behavior of the Ca^{2+} and Mg^{2+} ions during the sintering of alumina has been offered in terms of the entropy influence at higher temperatures and the ionic radius of the two cations.

References

1. Hansen, S. C. & Phillips, D. S., *Philosophical Magazine*, **A47**(2) (1983) 209.
2. Maier, J., *Solid State Ionics*, **18/19** (1986) 1141; Maier, J., In *Superionic and Solid Electrolytes: Recent Trends*, ed. A. L. Laskar & S. Chandra. Academic Press, New York, 1989, p. 137.
3. Maier, J., *J. Phys. Chem. Solids*, **46** (1985) 309.
4. Bousse, L., de Rooij, N. F. & Bergveld, P., *Trans. Electron. Dev.*, **30** (1983) 1263.
5. van den Berg, A., Bergfeld, P., Reinholdt, D. N. & Sudhälter, E. J. B., *Sensors Actuat.*, **8** (1985) 129; de Rooij, N. F., personal communication.
6. Maier, J., *Mat. Res. Soc. Symp. Proc.*, **135** (1989) 101.
7. Coble, R. L., *J. Appl. Phys.*, **32**(5) (1961) 793.
8. Mukhopadhyay, S. M., Jardin, A. P., Blakely, J. M. & Baik, S., *J. Am. Ceram. Soc.*, **71**(5) (1988) 358.
9. Cahn, J., *Acta Met.*, **10** (1962) 789.
10. Shaw, N. J. & Brook, R. J., *J. Am. Ceram. Soc.*, **69** (1986) 107.

11. Baik, S. & White, C. L., *J. Am. Ceram. Soc.*, **70**(9) (1987) 682.
12. Kaysser, W. A., Sprissler, M., Handwerker, C. & Blendell, J. E., *J. Am. Ceram. Soc.*, **70**(59) (1987) 339.
13. Berry, K. A. & Harmer, M. P., *J. Am. Ceram. Soc.*, **69** (1986) 143.
14. Moser, Z., Gasior, W. & Rzyman, K., *J. Electrochem. Soc., Electrochem. Sci. Technol.*, **129**(3) (1982) 55.
15. Sternberg, S. & Terzi, M., *J. Chem. Thermodynamics*, **30** (1971) 259.
16. Adamson, A. W., *Physical Chemistry of Surfaces*. John Wiley, New York, 1976.
17. Tasker, P. W., *Advances in Ceramics*, **10** (1984) 176.
18. Kingery, W. D., In *Introduction to Ceramics*, 2nd edn, ed. W. D. Kingery, H. K. Bowen & D. R. Uhlman. Wiley & Sons, New York, 1976, p. 183.
19. Rusanow, A. I., *Phasengleichgewichte und Grenzflächenerscheinungen*. Akademie-Verlag, Berlin, 1978, Chapter 17.

Appendix: The Free Energy of Wetting

Dupré's work of adhesion, which is often simply identified with the free energy of wetting, is defined by

$$W_{ad} = \gamma_{l/v} + \gamma_{s/v} - \gamma_{l/s} = \gamma_{l/v}(1 + \cos\theta) \quad \text{(A1)}$$

which indeed changes as $\gamma_{l/v}\cos\theta$:

$$\delta_s W_{ad} = \delta_s(\gamma_{l/v}\cos\theta) \quad \text{(A2)}$$

where the operator δ_s describes the variation in the surface crystallography. Since the total surface is not conserved during the wetting process, the real work of wetting, $\Delta_w G$, contains an additional term $(-\gamma_{l/v}\Delta A/a)$ and, due to the changes in the local pressure,[19] an additional factor of $\frac{1}{3}$. As a consequence $\Delta_w G$ changes as

$$\delta_s \Delta_w G = \tfrac{1}{3}\delta_s\left[\gamma_{l/v}\left(\cos\theta - \frac{\Delta A}{a}\right)\right] \quad \text{(A3)}$$

where a is the contact area (l/s) and ΔA is the change in the drop surface during wetting. Identifying the shape of the sessile drop with a spherical segment, it can be readily derived that $\Delta A/a$ changes as

$$\delta_s \frac{\Delta A}{a} = \delta_s\{(2 + A^2) - 4[\tfrac{1}{8}A(3 + A^2)]^{2/3}\} \quad \text{(A4)}$$

where

$$A \equiv \frac{1 - \cos\theta}{\sin\theta} \quad \text{(A5)}$$

which is not negligible with respect to $\delta_s\cos\theta$. Thus the ranking of $\Delta_w G$ as a function of temperature is not the same as that of the function $\gamma_{l/v}\cos\theta$ in Fig. 4.